OH EMISSION BANDS IN THE SPECTRUM OF THE NIGHT SKY. I

A. B. MEINEL
Lick Observatory and Yerkes Observatory
Received February 24, 1950

ABSTRACT

High-resolution spectra of the infrared night sky obtained at Yerkes Observatory have shown conclusively that the previously unidentified infrared emissions are due to the rotation-vibration spectrum of *OH*. The agreement between the vibrational spacing, the rotational constants, and the doublet structure of the emissions and the predicted *OH* structure is excellent. The observation of vibrational levels up to $v = 9$ shows that small inaccuracies exist in the currently accepted vibrational constants. A more accurate determination of these constants could be made, despite the low dispersion of the spectrograph. Other bands of this system of *OH* occur in the region of 1 μ and may account for the radiation detected by Stebbins, Whitford, and Swings, which has been attributed to N_2.

INTRODUCTION

Spectra obtained by the author[1] during 1948 at Lick Observatory with a grating spectrograph showed the presence of a large number of intense infrared radiations that exhibited a complex structure. From these earlier spectra, it was possible to identify only the *P* and *R* branches of the (0, 1) transition of the atmospheric system of O_2 at 8629 A and 8659 A, respectively.[2] The remaining radiations could not be attributed to any known band system of O_2, N_2, *NO*, *CO*, *CN*, CO_2, or H_2O. The present paper constitutes a continuation of these investigations.

INSTRUMENTATION

The spectrograph used in the current investigation, while similar to the spectrograph used for the observations at Lick Observatory, differed in several respects. The glass aspherical corrector plate was replaced by a fused-quartz corrector that had been optically figured to a high degree of accuracy. The low dispersion of the quartz, combined with the excellent figure, enabled a wider spectral range to be observed without deterioration of the images by the residual chromatic aberration of the corrector. The image size, determined visually, is less than 10 μ. Photographic star images as small as 12 μ have been obtained on Eastman III-C emulsions.

A collimator, loaned to the author by the California Academy of Sciences, was added to the spectrograph, in order to reduce the over-all length of the system. The achromatic collimator has an aperture of 6.5 inches and a focal length of 96 inches. The secondary spectrum produced by this lens, which was corrected for the visual region, was not found serious in the infrared. The large ratio of 18 between the collimator and the camera reduced the secondary spectrum by a factor of 324. The residual spectrum was then eliminated by a very slight tip of the plateholder.

The spectrograph was mounted on the base and yoke of a United States Navy searchlight. This mounting was made to enable the spectrograph to be pointed at any region of the sky for auroral studies. The image of the sky was projected on the slit of the spectrograph by means of a short-focal-length lens. This objective lens enabled a spectrum of the sky to be obtained along a vertical arc of 30°. A second lens of the same focal length as the objective lens was placed directly in front of the slit to serve as a field lens. All the transmission optical elements were low-reflection coated with magnesium fluoride. The

[1] *Pub. A.S.P.*, **60**, 357, 1948.

[2] A. B. Meinel, *Trans. Amer. Geophys. Union*, **31**, 21, 1950.

spherical mirror of the camera was coated with a hard layer of vacuum-deposited silver.

The spectrograph, as described above, has enabled high-resolution spectra of the night sky to be obtained with a relatively short exposure. The maximum exposure time employed was 12 hours. This exposure time differs greatly from the exposure times required for the studies at Lick Observatory. The 32-hour exposure at Lick Observatory compares to a 4-hour exposure at Yerkes Observatory. It is felt that the difference is not due to a greater sky brightness at Yerkes Observatory but to the observing techniques. The present spectrograph, although it has more optical elements, is more efficient. The largest factor in the increased efficiency, however, is attributed to the hypersensitization of the Eastman I-N emulsion.

The method of hypersensitization currently employed by the author is as follows:

Bathe 3 minutes in { water ..... 100 cc; ammonia (28%) ..... 8 cc; alcohol ..... 100 cc }
Rinse 2 minutes in pure alcohol
Dry in a cool air blast

This procedure yields plates of uniformly high sensitivity and negligible fog when precautions are taken to avoid contamination with chemical dusts present in all dark rooms.

Prior to exposure, each plate was pre-exposed to infrared light up to a density of 0.3. While this lowers the contrast, it provides a more accurate representation of the spectrum by removing the threshold inertia of the plate and by placing all features on the linear portion of the characteristic curve of the emulsion. This procedure has enabled an exposure of 12 hours to show the band structure out to 8960 A.

The spectrum plates were calibrated with a tungsten-lamp spectrum beside the comparison spectrum. In addition, an adjacent piece of the original I-N plate was calibrated in a spot and a spectral sensitometer to enable reduction of the emission intensities. It was found that the sensitivity of the hypersensitized emulsion was very constant from plate to plate when the preceding method of hypersensitization was used.

A comparison spectrum of krypton was first employed. This spectrum, however, is handicapped by having only a few intense lines in the infrared. A comparison spectrum of xenon was substituted, since it gives a large number of lines of varying intensity from 7000 to beyond 10,000 A.

OBSERVATIONS

The first plate taken with this spectrograph on December 29, 1949, showed immediately that the structure of several of the emission groups was similar. Since the camera was not in perfect focus, further details could not be noted with certainty. The plate of highest resolution, taken on January 10, 1950, showed clearly the detailed structure of each of the emission groups. An enlargement of this spectrum is shown in Figure 1. The hardness of the individual emissions on the longward side of each band group presented strong evidence that these emissions were, in fact, resolved spectral lines and not molecular bands. This fact demonstrated that the actual rotational structure of a band was being observed.

The measured wave lengths of the emissions from 7251.4 A to 8962.2 A are given in Table 1. There are no observed emissions as strong as intensity 2 between 6364 A and 7251 A. The faint bands in this region, reported by numerous authors, are diluted by the high dispersion of the grating spectrograph to such an extent that they are not detectable on short exposures. The intensities, as shown in Table 1, are corrected for the characteristic curve and the wave-length sensitivity of the emulsion. It is very interesting to note that the [*O* I] line at 6300 A is rather weak, compared to these *OH* bands.

IDENTIFICATION

The *P*, *Q*, and *R* branches could readily be identified for each group of emissions upon the assumption that the spectrum showed rotational structure. A preliminary analysis of

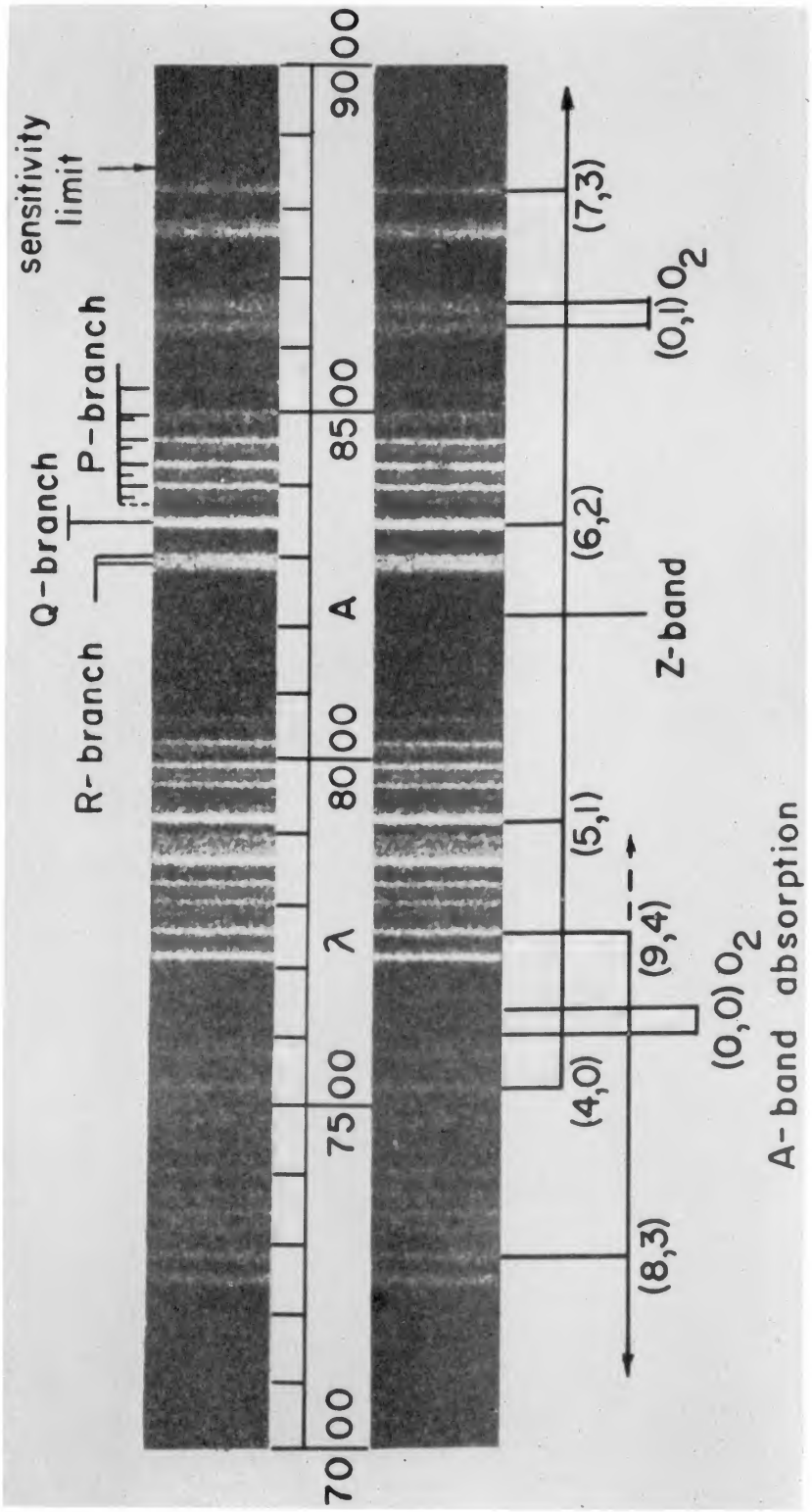

FIG. 1.—Infrared spectrum of the night sky, 7000–9000 A

TABLE 1

WAVE LENGTHS AND WAVE NUMBERS FOR EMISSION IN THE INFRARED SPECTRUM OF THE NIGHT SKY

λ (Air) A	ν (Vac) (Cm^{-1})	I	(v', v'') R, Q, P
6300.3	15868.3	8	O I
7251.4	13786.6	12	(8, 3)R
7284.2	724.5	12	(8, 3)Q
7323.6	650.7	5	(8, 3)P_1
7348.2	605.1	7	(8, 3)P_2
7375.8	554.2	5	(8, 3)P_3
7408.5	13494.3	4	(8, 3)P_4
7444.5	429.0	2	(8, 3)P_5
7481.8	365.8	7	(4, 0)R
7529.1	278.1	8	(4, 0)Q
7577.2	193.9	4	(4, 0)P_1
A-band	Absorption	.....	Region
7720.3	12949.2	28	(9, 4)R
7755.8	890.0	23	(9, 4)Q
7783.4	844.3	4	(9, 4)p_1
7799.0	818.6	17	(9, 4)P_1
7813.8	12794.4	5	(9, 4)p_2
7826.0	774.4	19	(9, 4)P_2
7857.8	722.6	57	(9, 4)P_3
7873.9	696.6		(5, 1)R
7892.6	666.7	7	(9, 4)P_4
7918.5	12625.2	42	(5, 1)Q
7952.6	571.0	5	(5, 1)p_1
7968.8	545.9	20	(5, 1)P_1
7983.8	521.9	8	(5, 1)p_2
7997.1	501.1	24	(5, 1)P_2
8018.7	12467.4	5	(5, 1)p_3
8029.7	450.3	19	(5, 1)P_3
8055.5	410.4	4	(5, 1)p_4
8066.1	394.2	12	(5, 1)P_4
8105.8	333.4	5	(5, 1)P_5
8289.8	12059.6	36	(6, 2)R
8300.0	044.8	31	(6, 2)R
8347.3	11976.6	74	(6, 2)Q
8384.8	923.6	8	(6, 2)p_1
8401.6	899.3	37	(6, 2)P_1
8418.0	11876.0	11	(6, 2)p_2
8432.3	855.9	44	(6, 2)P_2
8455.2	823.8	11	(6, 2)p_3
8467.4	806.8	35	(6, 2)P_3
8497.3	765.2	7	(6, 2)p_4
8506.7	11752.2	22	(6, 2)P_4
8544.9	699.7	4	(6, 2)p_5
8550.7	691.8	11	(6, 2)P_5
8594.4	632.2	5	(6, 2)P_6
8645.5	Minimum	(0, 1)	O_2 band
8778.4	11388.5	~210	(7, 3)R
8829.4	322.8	~200	(7, 3)Q
8889.3	246.4	~100	(7, 3)P_1
8923.7	203.1	~100	(7, 3)P_2
8962.2	154.9	~100	(7, 3)P_3

the strong lines of the P branch showed conclusively that the band was due to a hydride. The large values of $B_{v''} = 16$ cm^{-1} and $B_{v'} = 13$ cm^{-1}, combined with the doublet structure, limited consideration to the OH molecule.[3]

The grouping of the bands, as shown in Figure 1, indicated that the two emissions near 8800 A are the R and Q branches of another band. Subsequent exposures of longer duration have recorded the first three strong lines of the P branch, even though the sensitivity near 8900 is extremely low. The addition of this band and a very weak band at 7529 A made a total of six bands, of which four belong to one sequence and two to a second sequence.

VIBRATIONAL STRUCTURE

When the author communicated to Dr. Herzberg the foregoing results, together with a reproduction of the spectrum, Herzberg immediately noted that the two OH band sequences showed excellent coincidences with the extrapolated positions of the rotation-vibration bands of OH.[4] These coincidences were so striking that identification was almost certain, as surprising as this interpretation may seem in view of the large Δv-values. A subsequent analysis of the rotational structure by the author has confirmed this identification beyond any doubt. The values obtained by Herzberg, using the best-known values for the vibrational constants of OH, are shown in Table 2.

TABLE 2

COMPUTED AND OBSERVED BAND POSITIONS FOR OH

Sequence (v', v'')	λ (Comp) (A)	λ (Obs) (A)	Sequence (v', v'')	λ (Comp) (A)	λ (Obs) (A)
(4, 0)	7526	7529	(7, 3)	8850	8829
(5, 1)	7920	7918	(8, 3)	7293	7284
(6, 2)	8360	8347	(9, 4)	7762	7756

It is interesting that an extrapolation of the vibrational constants for OH derived from the ultraviolet electronic bands, which are only observed between low v-values, is satisfactory up to large v-values. The differences, however, are systematic and may indicate small errors in the accepted vibrational constants.

VIBRATIONAL CONSTANTS

Inasmuch as the predicted positions of the bands do not agree satisfactorily with the observed positions, a solution was made for new vibrational constants, with the observed data. The positions of the origin of the mean rotational band were extrapolated from the maximum of the strong observed Q branches.

The wave-number separation of the vibrational levels of a band system is given by the equation

$$\nu_v - \nu_{v+1} = \omega_e - 2\omega_e x_e (v+1) + 3\omega_e y_e (v+1)^2 + \dots , \tag{1}$$

neglecting a small constant term in $\omega_e y_e$. The wave number of the origin of a band corresponding to a transition between the levels v' and v'', then, is

$$(v' - v'')\,\omega_e - 2\omega_e x_e \sum_{v''}^{v'} (v+1) + 3\omega_e y_e \sum_{v''}^{v'} (v+1)^2 = \nu_{v',v''} . \tag{2}$$

[3] A. B. Meinel, *Ap. J.*, **111**, 207, 1950.

[4] Private communication.

When this expression was evaluated with the observed band origins, the following values were obtained by a least-squares solution:

$$\omega_e = 3721.9 \pm 0.5 , \qquad \omega_e x_e = 78.99 , \qquad \omega_e y_e = -0.235 .$$

The vibrational constants given above, however, do not fit two of the bands as shown in Table 3. This is apparently due to the blending of the (5, 1) Q branch with the P_5-line of the (9, 4) band in the one case. The Q branch of the (7, 3) band, on the other hand, is situated where the plate sensitivity is rapidly changing, thereby increasing the effective wave number of this branch.

TABLE 3

COMPARISON OF COMPUTED BAND POSITIONS USING NEW VIBRATIONAL CONSTANTS FOR *OH*

Sequence (v', v'')	ν (Comp) (Cm^{-1})	ν (Obs) (Cm^{-1})	$\delta\nu$ (O−C) (Cm^{-1})	Sequence (v', v'')	ν (Comp) (Cm^{-1})	ν (Obs) (Cm^{-1})	$\delta\nu$ (O−C) (Cm^{-1})
(4, 0).....	13288.8	13287.9	−0.9	(7, 3).....	11325.3	11332.6	+7.3
(5, 1).....	12639.9	12635.0	−4.9	(8, 3).....	13738.3	13735.7	−2.6
(6, 2).....	11985.5	11986.4	+0.9	(9, 4).....	12902.6	12901.2	−1.4

ROTATIONAL STRUCTURE

An analysis of the rotational structure of the *OH* bands confirms the interpretation indicated by the vibrational spacing. Figure 2 shows the observed line positions in the (5, 1) 7918 A band and the (6, 2) 8347 A band. The strong P branch and the weak P branch lines were combined in the manner indicated in Figure 2, in order to determine more accurately the rotational constants and the band origin according to the following equation:

$$P(K) = B_{v'} - B_{v''}) K^2 - (B_{v'} + B_{v''}) K + \ldots . \tag{3}$$

The rotational constants are related to the observed first (Δ') and second (Δ'') differences by the equations

$$B_{v'} + B_{v''} = \Delta' - \bar{\Delta}''(K + \tfrac{1}{2}) , \tag{4}$$

$$B_{v'} - B_{v''} = \bar{\Delta}'' . \tag{5}$$

Table 4 shows the values obtained for the (5, 1) and (6, 2) bands.

DOUBLET SPLITTING

The doublet structure of the bands is very noticeable in Figure 1, although the reproduction of the spectrum loses considerable faint detail. Hill and Van Vleck[5] have given a theoretical expression for the doublet splitting for cases intermediate between Hund's case *a* and case *b* states. The parameter in this expression is the ratio between the separation, A, of the $^2\Lambda_{\Lambda+1/2}$ and $^2\Lambda_{\Lambda-1/2}$ states and the rotational constants, B_v. In terms of the J-values, we have

$$F_{1\atop 2}(J) = B_v\{(J + \tfrac{1}{2})^2 - \Lambda^2 \mp \tfrac{1}{2}[4(J + \tfrac{1}{2})^2 + Y(Y - 4)\Lambda^2]^{1/2}\} + \ldots , \tag{6}$$

[5] *Phys. Rev.*, **32**, 250, 1928.

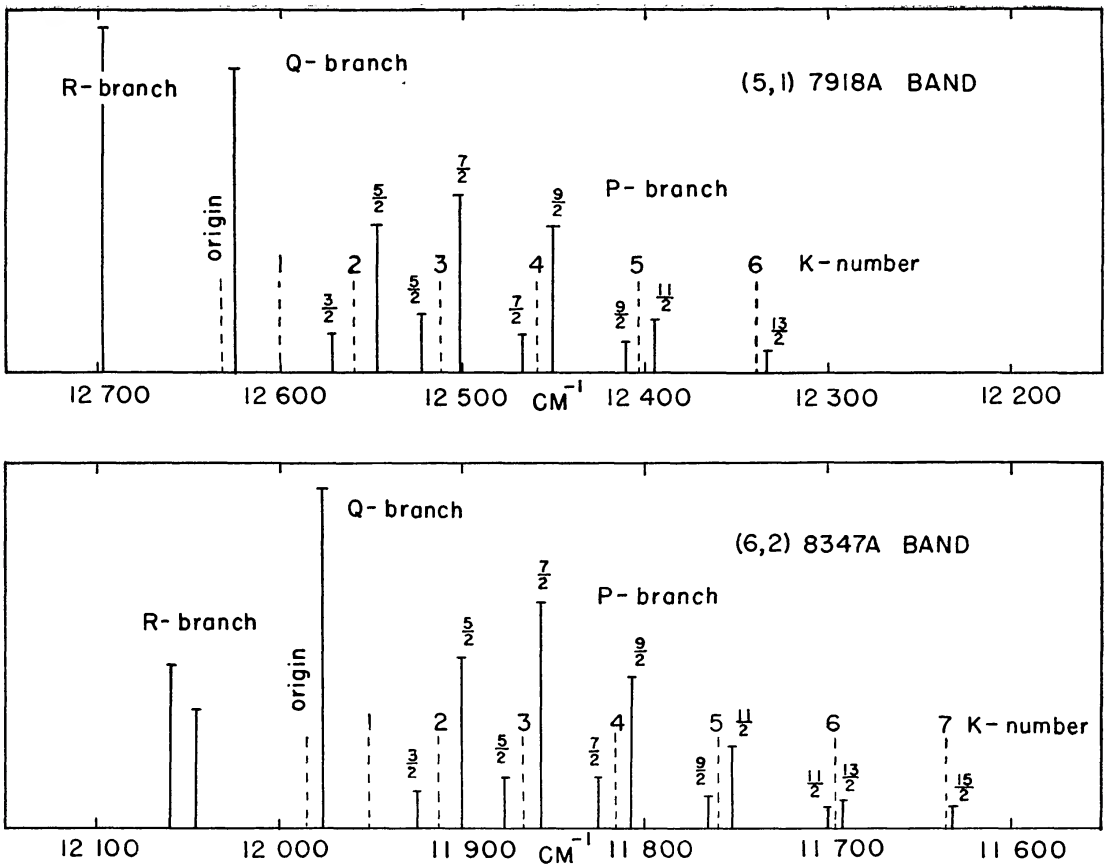

FIG. 2.—Observed line positions for the night-sky *OH* bands

TABLE 4

DETERMINATION OF ROTATIONAL CONSTANTS FOR THE *OH* BANDS

	(5, 1) 7918 A BAND			(6, 2) 8347 A BAND		
K.....	Δ' (Cm^{-1})	Δ'' (Cm^{-1})	$(B_{v'}+B_{v''})$ (Cm^{-1})	Δ' (Cm^{-1})	Δ'' (Cm^{-1})	$(B_{v'}+B_{v''})$ (Cm^{-1})
2.....	−47.0		33.3	−45.2		31.5
		−5.6			−5.4	
3.....	−52.6		33.4	−50.6		31.4
		−4.0			−6.0	
4.....	−56.6		31.9	−56.6		31.9
					−6.4	
5.....	.....		.....	−63.0		32.8
Average $(B_{v'}+B_{v''})$			32.9			31.9

	$B_{v'}$	$B_{v''}$	$B_{v'}$	$B_{v''}$
Observed.....	15.1	17.8	14.6	17.3
Computed.....	15.0	17.8	14.4	17.1

where $Y = \Delta/B_v$. The equation for a P branch of the $^2\Pi$ transition ($\Lambda = 1$), then, is

$$P_{\frac{1}{2}}(J) = {}^1\Pi(J) \mp \frac{B_{v'}}{2}\,[4(J-\tfrac{1}{2})^2 + Y'(Y'-4)]^{1/2} \pm \frac{B_{v''}}{2}\,[4(J+\tfrac{1}{2})^2 + Y''(Y''-4)]^{1/2} + \ldots = {}^1\Pi(J) \mp \delta(J), \tag{7}$$

where $^1\Pi(J)$ refers to the positions of a singlet P branch for half-integer J-values. The last term represents the doublet splitting of the F_1 and F_2 components for lines of equal J. The doublet splitting about the position of the lines defined by $F(K) = B_vK(K+1) + \ldots$ is related to the J-splitting by

$$\begin{aligned} P_1(K) &= {}^1\Pi(K) + \{(B_{v'} - B_{v''})K + \tfrac{1}{4}(B_{v'} + 3B_{v''}) - \delta(J = K + \tfrac{1}{2})\} \\ P_2(K) &= {}^1\Pi(K) - \{(B_{v'} - B_{v''})K - \tfrac{1}{4}(3B_{v'} + B_{v''}) - \delta(J = K - \tfrac{1}{2})\}. \end{aligned} \tag{8}$$

The computed and observed values of the doublet splitting are compared in Table 5 and

TABLE 5

COMPARISON OF THE OBSERVED AND COMPUTED DOUBLET SPLITTING FOR *OH*

J	$\delta(J)_{comp}$ (Cm^{-1})	$\delta(J)_{obs}$ (Cm^{-1})	K	$\overline{\delta(K)}_{comp}$ (Cm^{-1})	$\overline{\delta(K)}_{obs}$ (Cm^{-1})
$\frac{3}{2}$	± [7.9]	± [7.1]	2	±11.6	±12.3
$\frac{5}{2}$	12.1	11.6	3	10.0	10.2
$\frac{7}{2}$	16.3	16.0	4	8.8	8.5
$\frac{9}{2}$	20.4	20.8	5	7.6	6.8
$\frac{11}{2}$	±24.2	±26.2	6	±6.6	± 5.4

Figure 3 for the (5, 1) 7918 A and (6, 2) 8347 A bands, using the value $A = -138.3\ cm^{-1}$. For *OH*, the splitting F_1 refers to the $^2\Pi_{3/2}$ component, and the splitting F_2 refers to the $^2\Pi_{1/2}$ component. The parentheses about the $\delta J(\frac{3}{2})$ term indicates that $J = \frac{1}{2}$ is missing in the $^2\Pi_{3/2}$ state. This quantity refers to the position of the missing component as obtained from the series for the intense P branch (F_1).

FAR INFRARED *OH* BAND POSITIONS

With the conclusive identification that the strong night-sky emissions are due to the rotation-vibration bands of *OH*, it is possible to utilize the vibrational constants to predict the positions of the sequences of this band system. The most striking fact about the observed bands is that they have large Δv-values, the two sequences being for $\Delta v = 4$ and 5. If the vibrational motion of a molecule is strictly harmonic, the selection rule for transitions is $\Delta v = \pm 1$. It is only for anharmonic oscillators that this selection rule can be violated. For such an oscillator, transitions with $\Delta v = 1, 2, 3, \ldots$, may occur; however, the transition probability rapidly decreases with an increase in Δv. Since the wave functions have not been computed for the *OH* state at the present time, it is not possible to evaluate the transition probabilities. It is certain, however, that the bands in the unobservable infrared must be much more intense than those currently observed in the photographic region.

The author has held the opinion for some time that an extension of this band system in the infrared could account for the 10440 A radiation of Stebbins, Whitford, and Swings. This suggestion has now been made independently by Herzberg. The identification of the 10440 A radiation by Swings as due to the (0, 0) band of the first positive sys-

tem of N_2 has been widely accepted, although it has not been possible to explain the absence of Vegard-Kaplan bands from $v' = 0$.

An observation by Meinel and Smith at Lick Observatory in November, 1949, gave evidence that the emission near 10400 A was not even approximately monochromatic. The observation was made by placing a red-sensitive photocell behind a slit in the focal plane of the spectrograph. The night-sky spectrum was scanned from approximately 11000 A to 7000 A with an equivalent slit-width of 300 A. The level of intensity was observed to be high at the long-wave-length limit of the photocell at 11000 A. The intensity level decreased uniformly with decreasing wave length, with a minor maximum

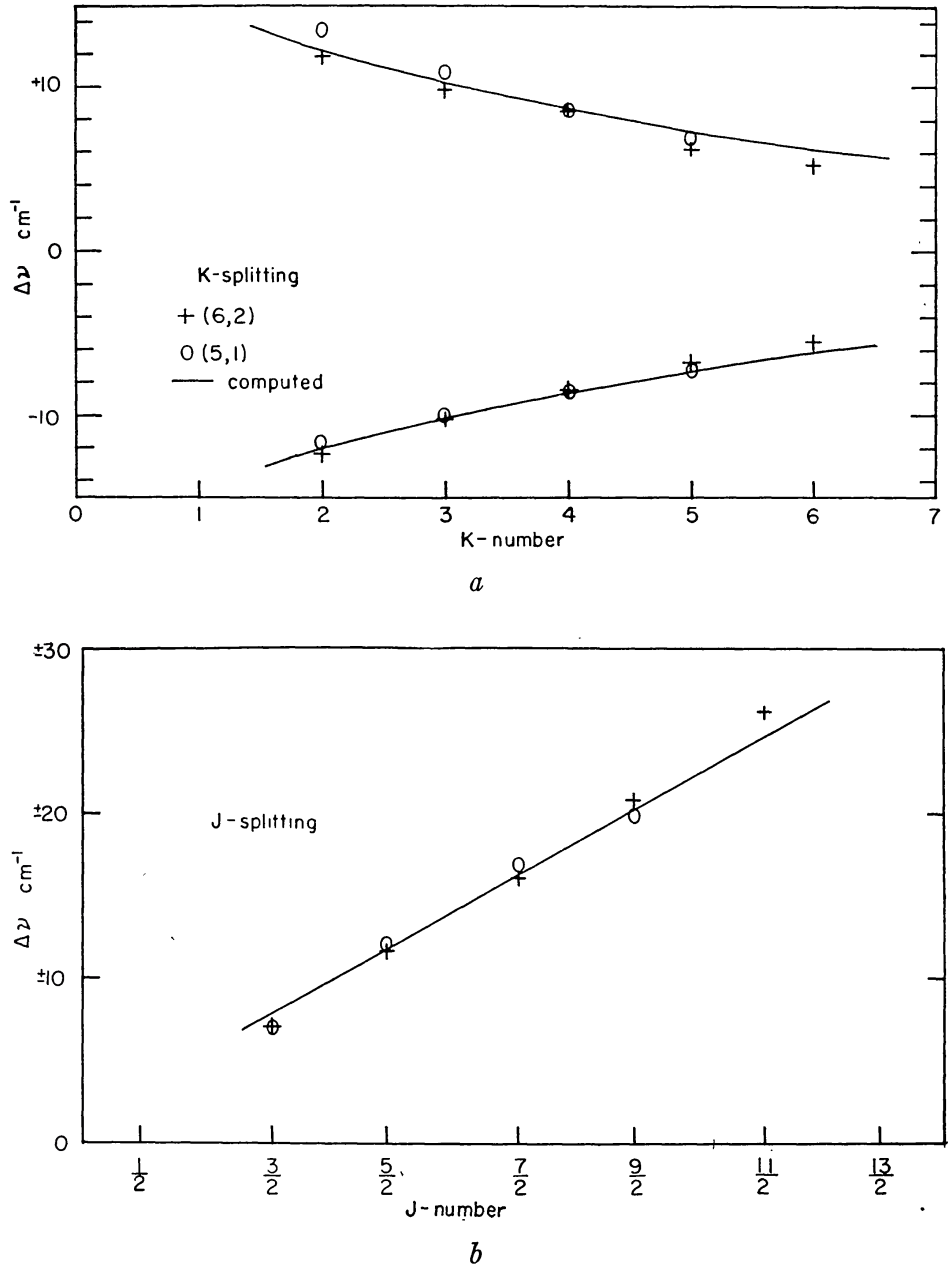

FIG. 3.—Observed doublet splitting of the night-sky *OH* bands

near 8000 A. This observation strongly indicated that numerous radiations were present beyond 9000 A. A more accurate photoelectric scanning of the spectrum is planned for the near future.

The origins for a large number of *OH* bands are given in Table 6 and Figure 4. The lengths of the lines in Figure 4 are arbitrary. Lines originating from levels 8 and 9 appear to be the strongest and are indicated by longer lines. It is interesting to note that the strongest member of the $\Delta v = 4$ sequence occurs at 10014 A. Overlapping this radiation are the bands of the $\Delta v = 3$ sequence. The sensitivity-curve of the filter and photocell used by Stebbins, Whitford, and Swings is plotted in Figure 4. This diagram shows that the 10440 A radiation may be attributed to a large number of very strong *OH* bands.

TABLE 6

OH BAND POSITIONS

$\Delta v = 1$	$\Delta v = 2$	$\Delta v = 3$
(9, 8) 2243.0 cm^{-1}	(9, 7) 4656.0 cm^{-1}	(9, 6) 7237.5 cm^{-1}
4.458 μ	2.148 μ	13817 A
(8, 7) 2413.0	(8, 6) 4994.5	(8, 5) 7743.2
4.144	2.002	12915
(7, 6) 2581.5	(7, 5) 5330.2	(7, 4) 8244.6
3.874	1.876	12129
(6, 5) 2748.7	(6, 4) 5663.1	(6, 3) 8741.8
3.638	1.777	11439
(5, 4) 2914.4	(5, 3) 5993.1	(5, 2) 9234.7
3.431	1.668	10829
(4, 3) 3078.7	(4, 2) 6320.3	(4, 1) 9723.5
3.248	1.582	10284
(3, 2) 3241.6	(3, 1) 6644.8	(3, 0) 10208.0
3.085	1.505	9796
(2, 1) 3403.2	(2, 0) 6966.4	
2.938	1.436	
(1, 0) 3563.2		
2.806		

$\Delta v = 4$	$\Delta v = 5$	$\Delta v = 6$
(9, 5) 9986.2 cm^{-1}	(9, 4) 12900.6 cm^{-1}	(9, 3) 15979.3 cm^{-1}
10014 A	7752 A	6258 A
(8, 4) 10657.6	(8, 3) 13736.3	(8, 2) 16977.9
9383	7280	5890
(7, 3) 11323.3	(7, 2) 14564.9	(7, 1) 17968.1
8831	6867	5565
(6, 2) 11983.4	(6, 1) 15386.6	(6, 0) 18949.8
8345	6500	5277
(5, 1) 12637.9	(5, 0) 16201.1	
7913	6172	
(4, 0) 13286.7		
7526		

These conjectures do not mean that the (0, 0) band of the first positive system of N_2 is completely absent. Stebbins, Whitford, and Swings observed fluctuations in the photoelectric deflection, while the near-infrared *OH* bands appear to be quite constant from night to night. Since infrared N_2 first positive bands appear with great intensity during auroral disturbances,[2] the fluctuations observed by the above authors may have been due to the abnormal excitation of the (0, 0) band.

VISIBLE REGION *OH* BAND POSITIONS

An examination of spectra obtained by H. W. Babcock,[6] Slipher,[7] and Sommer[7] shows the presence of the *OH* bands in the visible region of the night-sky spectrum. The very conspicuous emission on the shortward side of 6300 A on the spectrum published by Babcock, at 6258 A, corresponds to the strongest band of the $\Delta v = 6$ sequence at 6258.1 A (9, 3). This and the other coincidences are shown in Table 7. The

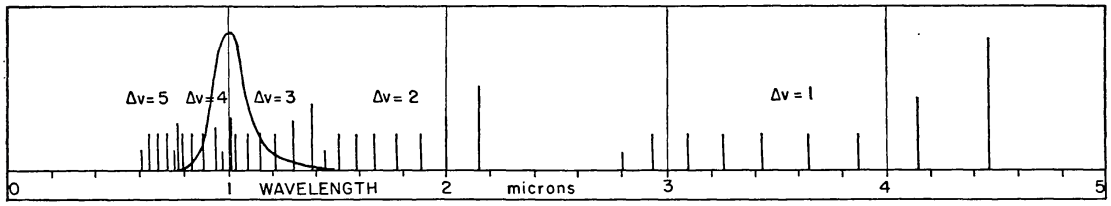

FIG. 4.—*OH* band positions in the infrared

TABLE 7

OBSERVED *OH* BANDS IN THE VISIBLE REGION

Babcock	Slipher	Sommer	*OH* Bands	Babcock	Slipher	Sommer	*OH* Bands
.....	7270	7290	(8, 3) 7280	6502	.....	.....	(6, 1) 6500
.....	6870	6863	(7, 2) 6867	6258	.....	.....	(9, 3) 6258

weak emission at 6502 A was not observed by Slipher or Sommer, while the 6258 A emission was too near to the intense 6300 A line to be observable except with the higher dispersion employed by Babcock. The emissions (8, 2) and (7, 1) would be much fainter and difficult to detect, inasmuch as they very nearly coincide with *Na* I at 5893 A and [*O* I] at 5577 A. The presence of the *OH* band system in the red region of the night-sky spectrum consequently eliminates a number of identifications ascribed to the first positive system of N_2. A detailed discussion of the intensity characteristics of the rotational and vibrational structure, as related to an excitation mechanism, will be presented in a following paper.

In conclusion, the author wishes to express his special indebtedness to Dr. Gerhard Herzberg for his instant recognition that the *OH* bands were due to the rotation-vibration spectrum of *OH*. This investigation has been sponsored by the Office of Naval Research in co-operation with the Lick Observatory and the Yerkes Observatory.

Note added in proof.—The author has received a private communication from J. Dufay, announcing independently the observation of the *OH*-band system in the visible region. An additional discussion of the *OH* bands in the visible region, with respect to previous identifications with the first positive bands of N_2 and $H\alpha$, is given in the March issue of the *Astrophysical Journal*.

[6] *Pub. A.S.P.*, **51**, 47, 1939.

[7] C. Fabry, J. Dufay, J. Cojan, *Étude de la lumière du fond du ciel nocturne* ("Éditions rev. d'opt." [Paris, 1934]).